

*Letter to the Editor***The X-ray jet in the merging galaxy system Markarian 266\***

W. Kollatschny and P. Kowatsch

Universitäts-Sternwarte Göttingen, Geismarlandstrasse 11, D-37083 Göttingen, Germany

Received 4 May 1998 / Accepted 11 June 1998

**Abstract.** We present deep ROSAT X-ray images of the double nucleus galaxy Mrk 266 in combination with optical images and spectra. The High Resolution Imager (HRI) X-ray morphology can be divided into four components: two nuclei of the merging galaxies, a diffuse galactic component and a strong northern jet coincident with very strong optical line emission. This jet component is decoupled from the rest of the merging system considering the internal kinematics. The luminous X-ray jet is excited by hot postshock gas with respect to the morphology, the high excitation emission lines and the kinematics.

**Key words:** galaxies: individual(Mrk 266) – galaxies: Seyfert – galaxies: interactions – X-rays: galaxies

**1. Introduction**

Markarian 266 is a nearby merging galaxy system (Petrosian, 1980) of two former spiral galaxies. The UV/optical spectra of the individual nuclei have been classified to be of Seyfert 2 (south-west) and Liner (north-east) type (Kollatschny et al., 1984; Osterbrock et al., 1983). Further detailed investigations of this infrared-luminous system have been published by Hutchings et al.(1988) and Mazzarella et al.(1988); they detected a third radio component between the two optical nuclei. Wang et al.(1997) discussed additional starburst properties of this system in context with medium-deep X-ray observations.

**2. Observations and data reduction**

We took deep ROSAT observations of Mrk 266 with the HRI over the time period June 28th to July 6th, 1996, with a total integration time of 39,740 seconds. During our long-term observing run the background X-ray flux was very low:  $2.9 \text{ cts ksec}^{-1} \text{ arcmin}^{-2}$ . Further archival X-ray data will not be taken into account; these images differ in a not reproducible way for individual satellite orbits causing a spurious extent in the co-added image. Additionally, we obtained multicolour optical images as well as spectra at various opportunities. Optical

Send offprint requests to: W. Kollatschny

\* Based on observations taken with ROSAT, at Calar Alto Observatory, with HST, and with the VLA

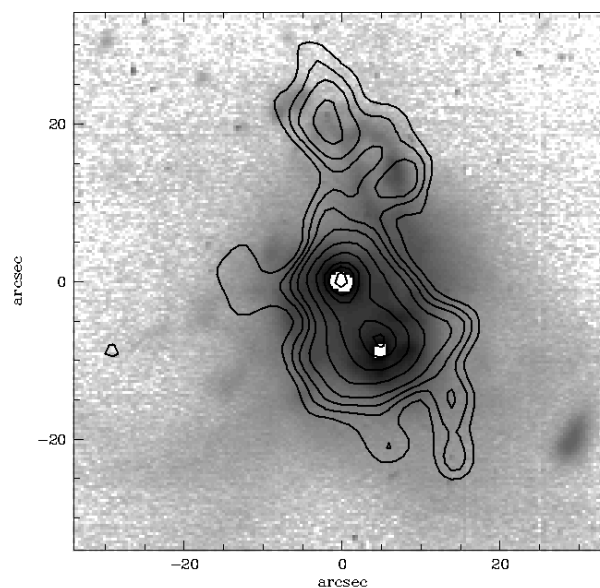


**Fig. 1.** ROSAT HRI X-ray contour levels overlaid on an optical V-band image of Mrk 266. The X-ray data (exp.time: 39,740 s) have been smoothed with a Gaussian filter of 5 arcsec FWHM. The contour levels are at 5,7.5,10,13,20,30,40,45,50  $\sigma$ . North is to the top; east is to the left.

B,V,R-images of Mrk 266 were taken under photometric conditions with the 2.2m telescope at Calar Alto observatory. The observations were made under seeing conditions of 1.0 - 1.2 arcsec. Our exposure times amounted to 3,600 s (Johnson B), 1,800 s (Johnson V) and 480 s (Johnson R), respectively. The pixel scale of the RCA-chip corresponds to  $0.351 \times 0.351$  arcsec. The original images were aligned better than 0.1 pixel for the generation of B-V,B-R and V-R difference images. In Fig. 1 the V-band image and in Fig. 2 the V-R image of Mrk 266 are shown with the HRI X-ray contour levels overlaid. We present an optical spectrum obtained with the Calar Alto 3.5 m telescope. A RCA-chip (1024x640) was attached at the Boller and Chivens spectrograph. The spectrograph slit had a projected width of 2 arcsec and length of about 2 arcmin. We covered the wavelength range from 3700–7100 Å with a spectral resolution of 3.4 Å per pixel. An archival HST image taken with WFPC 2 is shown

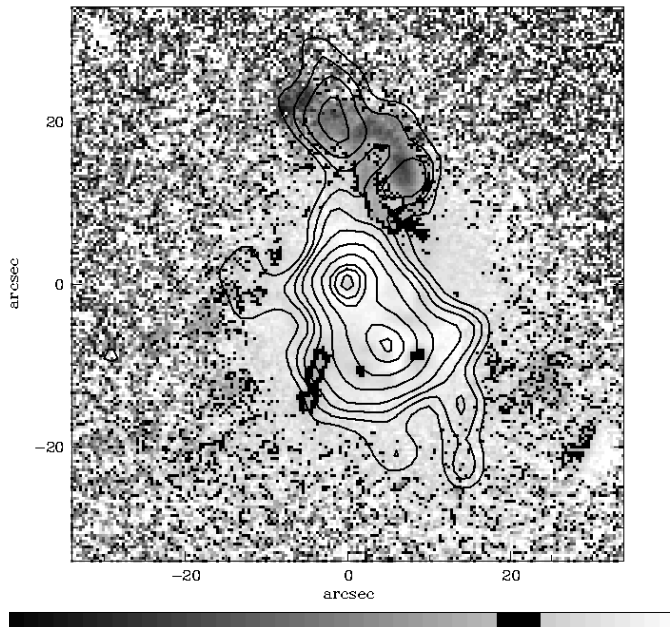


**Fig. 2.** V-R colour image of Mrk 266. Overlay of X-ray contour levels as in Fig. 1.

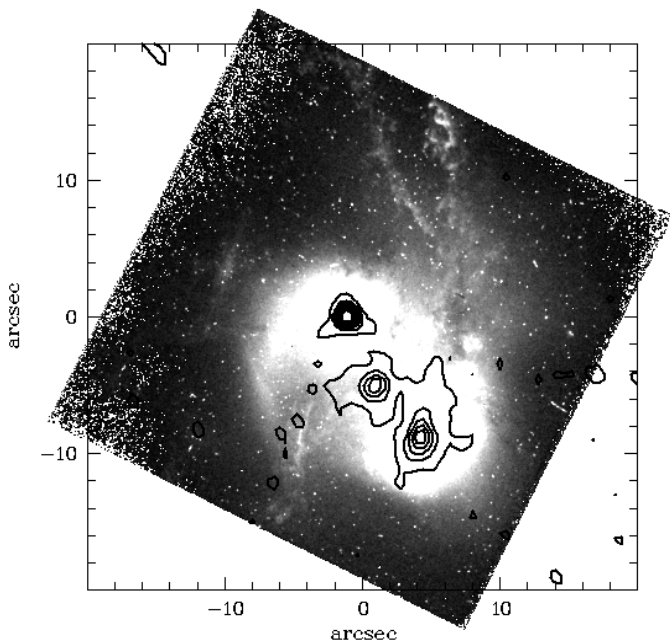


**Fig. 3.** WFPC2 HST observations of Mrk 266 with overlay of radio contours (VLA 20cm). North is up; east is to the left.

in Fig. 3. The observing time amounted to 500 sec. The image was taken with the broad band filter F606W integrating the flux from 4700 - 7200 Å. We obtained high-resolution radio observations at 6 cm and 20 cm with the VLA in the snapshot mode in the extended A configuration. The beam-width (HPBW) was  $0.''35 \times 0.''35$  at 6 cm and  $1.''2 \times 1.''2$  at 20 cm. Our radio maps are similar to those obtained by Hutchings et al.(1988) and Mazzarella et al.(1988).

### 3. Results

#### 3.1. X-ray and optical morphology

Our HRI X-ray contour levels – smoothed with a Gaussian filter of 5 arcsec FWHM – are plotted over the V-band image of Mrk 266 in Fig. 1. One can distinguish four components in the X-ray image: two compact nuclei separated by 10 arcsec, a diffuse component of the merging system ( $33'' \times 28''$  box) and a northern jet component ( $25'' \times 30''$  box). During our 40 ksec observing run we obtained the following count rates:  $66 \pm 8$  counts (north-eastern component, 10 arcsec ring),  $78 \pm 9$  counts (south-western component, 10 arcsec ring),  $311 \pm 18$  counts ( $33'' \times 28''$  box, integrated system without the jet) and  $120 \pm 11$  counts (northern jet,  $25'' \times 30''$  box). The individual HRI components are not resolved with the ROSAT PSPC detector (30 arcsec spatial resolution). Tests with single component models gave unsatisfactory fits to the observed PSPC spectrum (Wang et al., 1997). The integrated PSPC X-ray luminosity of Mrk 266 comes to  $1.1 \cdot 10^{42}$  ( $7 \cdot 10^{41}$ – $2.6 \cdot 10^{42}$ ) erg/s. Assuming the relative number of HRI counts is directly proportional to their share of the integrated X-ray flux we work out the following X-ray luminosities of the individual components (in units of  $10^{41}$  erg/s): north-eastern nucleus: 1.65, south-western nucleus: 2.0, diffuse component without the nuclei and the jet region: 4.3, northern jet: 3.1.

The dominating X-ray jet structure begins 15 arcsec north of the SW-nucleus and extends as far as 24 arcsec in north-east direction. This corresponds to a projected length of 13.2 kpc for the galactic radial velocity  $v_r = 8280 \text{ km s}^{-1}$  ( $H_0 = 75 \text{ km s}^{-1} \text{ Mpc}^{-1}$ ). An even more striking similarity can be found between the X-ray structure of the northern jet and the B-V, B-R and V-R images (Fig. 2). The V-R colour is quite homogeneous over the merging galaxy system ( $V-R = 0.5 \pm 0.1$ ) but exceptionally blue in the northern jet region ( $V-R = -0.25 \pm 0.2$ ). The correspondence between the optical and X-ray jet morphology indicates their same physical origin. One can recognise a bubble like structure in the jet of 14 arcsec length (7.7 kpc) and 7 arcsec width (4. kpc) in the optical due to the better spatial resolution. While the V-R colour of this northern jet component is exceptionally blue due to the intensive [OIII] $\lambda$  5007 line emission the B-V colour ( $B-V = 1.2 \pm 0.1$ ) is very red on the other hand.

The two nuclei have a distance of 10.3 arcsec in the HST image as well as in our VLA radio image. This corresponds to a projected distance of 5.67 kpc. The north-eastern Liner component is more compact in all frequencies from radio (VLA), opt.(HST, ground based), UV (IUE) to X-ray (ROSAT) in comparison to the south-western Seyfert nucleus.

It has been mentioned by Mazzarella et al.(1988) and Hutchings et al.(1988) that a third VLA radio component is located in between the optical nuclei nearly exactly on the connecting line between the outer components (see Fig. 3). No counterpart of the central radio component can be detected in the X-ray image and in the HST image within a 1 arcsec radio error-box. This central radio component is located at a huge s-shaped bipolar jet-like structure extending 13.5 arcsec (7.7 kpc) to the south-east and 12.5 arcsec (7.1 kpc) to the north-west where it leads

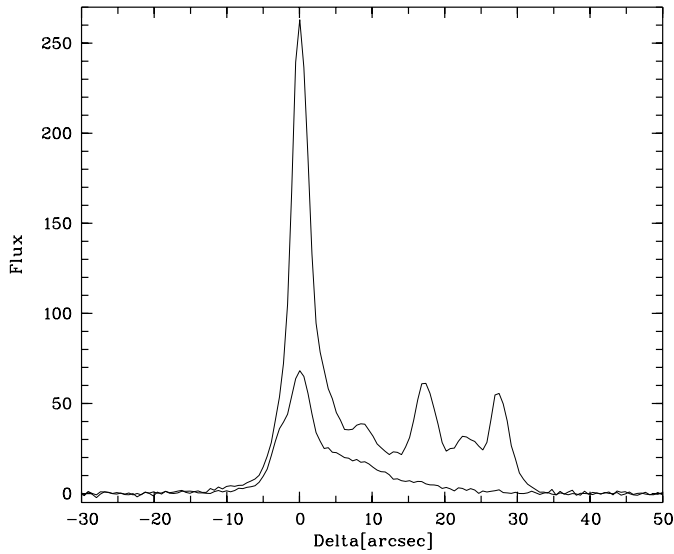


**Fig. 4.** Intensity tracing along the slit in north-south direction in the [OIII] $\lambda$  5007 line (4991–5023Å; upper curve) and in the adjacent continuum (5042–5074Å; lower curve).

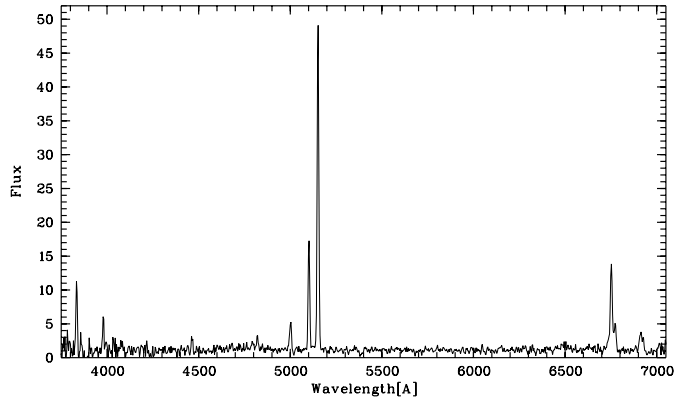


**Fig. 5.** Optical spectrum of the integrated jet region of Mrk 266

into the extended X-ray jet. The s-shaped structure is to be seen in the HST image (Fig. 3) and in the ground based [OIII] $\lambda$ 5007 image (e.g. Hutchings et al., 1988). This double structure can be recognised partly in the V-R image (Fig. 2), too. The inner jet draws to a helical structure considering the white filaments (Fig. 3).

### 3.2. Spectral Diagnostics and Kinematics

We took spectra with the slit in north-south direction passing the south-western nucleus and the northern jet region. Fig. 4 shows spatially resolved intensity tracings of the [OIII] $\lambda$  5007 line (4991–5023 Å) and the neighbouring continuum (5042–5074 Å). This pattern is typical for all emission line and continua tracings: the northern jet structure seen in the broad band images originates only from line emission; it is not present in the stellar continuum.

An integrated optical spectrum over the X-ray jet region is shown in Fig. 5. The excitation degree - derived from the line

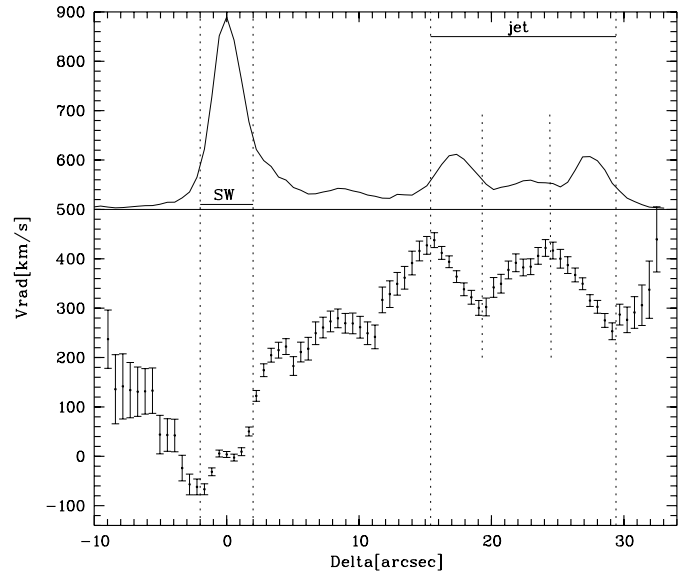


**Fig. 6.** Radial velocity of the [OIII]-line along the spectral slit. For comparison the [OIII]-intensity after subtraction of the continuum has been plotted in the upper part.

ratios HeII $\lambda$  4686/H $\beta$  and [NeIII] $\lambda$  3869/[OII] $\lambda$  3727 - is highest in the jet region (0.33 resp. 0.41) in comparison to other internal galaxy spectra (0.17 resp. 0.11). Furthermore, the intensities of the [OIII] $\lambda$  5007,4959 lines are exceptionally strong with respect to H $\beta$  and H $\alpha$ .

Earlier observations have shown that the velocity field of Mrk 266 is highly disturbed due to the merging process (e.g. Hutchings et al., 1988; Kollatschny, 1990). In Fig. 6 we present the projected gaseous velocities in north-south direction derived from the [OIII] $\lambda$  5007 line.

The velocities have been normalized to  $v_{\text{rad}} = 0 \text{ km s}^{-1}$  at the south-western Seyfert nucleus. The velocity field in the northern jet region is decoupled from the rest of the interacting galaxy system. Furthermore, at the border of the filamentary structures (enhanced [OIII]-intensities) the velocities show a constant gradient in the same direction on both sides.

## 4. Discussion

Read and Ponman (1997) investigated in detail X-ray properties of a larger sample of nearby spiral galaxies. The integrated X-ray luminosity of all their sample galaxies was less than  $\log L_X = 40.78$ . In a further paper (Read & Ponman, 1998) they determined the X-ray luminosities of prominent merging galaxies in different evolutionary stages: the integrated X-ray luminosities amounted to  $\log L_X = 41.18$  at the most. In contrast, the X-ray luminosity of the northern jet in the Mrk 266 system ( $\log L_X = 41.49$ ) is higher than the integrated X-ray luminosities of all the merging galaxies. Furthermore, the X-ray luminosity in the Mrk 266 jet is a factor of ten higher than that of known X-ray jets in galaxies e.g. M87 (Biretta et al., 1991) and of typical galactic super-winds in e.g. M82 (Read and Ponman, 1997). There might be known one

extragalactic system showing similar X-ray properties: the interacting galaxy group Stephan's Quintet (Pietsch et al., 1997). But the opt./X-ray morphology is slightly different.

No data have been published so far about interacting/merging galaxies with tidal arms showing comparable V-R colours and/or X-ray fluxes. We are investigating a larger sample of interacting galaxies with active nuclei: none of these shows as extreme properties.

We discuss four possibilities to explain the extra-nuclear X-ray emission in the northern region: starburst in an extra-nuclear region; excitation from one of the active nuclei; 'central' starburst with super-wind; photoionisation by a fast shock.

A starburst in a tidal arm region is extremely unlikely: there is no indication for an underlying stellar/starburst component in the continuum flux. The X-ray flux is too high to be explained by a reasonable number of SN ( $\log L_X = 33.-36.$ ) and X-ray binaries ( $\log L_X = 37.5-38.5$ ). Furthermore, the optical/ X-ray morphology and the gas velocities do not support this picture.

Photoionisation by the southern Seyfert nucleus is very unlikely since the excitation of the optical spectra is lower in the intermediate region between the Seyfert nucleus and the jet.

The explanation of the X-ray jet by a super-wind model caused by a central starburst is unlikely, too, because of the non-radial geometry. The opening angle of the X-ray/ [OIII] emission region in Mrk 266 is much smaller in comparison to other known bipolar wind outflows (Suchkov et al., 1994). Additionally, one would expect a radial velocity gradient; this is not to be seen in the emission region of the jet. Wang et al. (1997) preferred the super-wind model to explain their observations of Mrk 266; but their X-ray image was not deep enough to detect the jet and they had no information about spectra and kinematics in the X-ray jet. Furthermore, the X-ray intensity in the jet is too strong to be explained by a super-wind in comparison to other galaxies showing this phenomenon.

Taking into account the optical line intensity ratios, the optical and X-ray morphology, and the X-ray luminosity in Mrk 266, the most plausible mechanism explaining the X-ray jet is excitation by hot postshock gas caused by fast shocks emitting EUV/soft X-ray radiation (Bremsstrahlung) and photoionising the gas (Dopita & Sutherland, 1996). The X-ray jet is redshifted by  $300 \text{ km s}^{-1}$  with respect to the innermost galactic region. On the other hand the velocity structure within the jet in south-north direction shows no further outflow signs but solid body rotation of the outer filamentary regions. This might be explained by

a helical motion of the jet. The morphology seen on the HST image supports this idea. On spectra taken along the major axis of the jet it turns out that the gaseous velocity field is retarded at the end of the jet. The large scale curved structure of the jet seen in the HST and X-ray images is likely to be caused by precessional motions of the merging system.

It is not clear where the energy source generating the jet is located. The HST image supports the idea that the jet originates at the central radio source between the two optical nuclei. On the other hand no optical or near-infrared K-band counterpart (McLeod and Rieke, 1995) has been found so far. Mazzarella et al. (1988) proposed that the central radio emission is produced by synchrotron emission stimulated by the collision of two merging galaxies. But the question regarding the energy source of the jet needs further detailed investigations. The jet might be generated in the outer parts of the prograde interacting disks of system. With time more energy is added and eventually elongates the direction of the steepest density and pressure gradients. During the break out process the disk might play an important role in focusing the flow in the direction of the steepest density and pressure gradients out of the merging system. The high-velocity jet drives a shock into the halo gas leading to X-ray emission at the shock interaction region.

*Acknowledgements.* We thank K. Bischoff and P. Papaderos for useful comments. This work has been supported by DARA grant 50 OR94089 and DFG grant Ko 857/13-2.

## References

- Biretta J.A., Stern C.P., & Harris D.E., 1991, AJ, 101, 1632
- Dopita M.A., & Sutherland R.S., 1996, ApJS, 102, 161
- Hutchings J.B. et al., 1988, AJ, 96, 1227
- Kollatschny W., 1990, IAU Coll. 124, ed. : Sulentic et al., p. 221
- Kollatschny W., & Fricke K., 1984, A&A, 135, 171
- Mazzarella J.M. et al., 1988, ApJ, 333, 168
- McLeod K.K., & Rieke G.H., 1995, ApJ, 441, 96
- Osterbrock D.E., & Dahari O., 1983, ApJ, 273, 478
- Petrosian A.R. et al., 1980, Astrofizika, 16, 621
- Pietsch W. et al., 1997, A&A, 322, 89
- Read A.M., & Ponman T.J., 1997, MNRAS, 286, 626
- Read A.M., & Ponman T.J., 1998, MNRAS, in press
- Suchkov A.A. et al., 1994, ApJ, 430, 511
- Wang J. et al., 1997, ApJ, 474, 659